Soft Matter

View Online / Journal Homepage / Table of Contents for this issue

Dynamic Article Links

Cite this: *Soft Matter*, 2012, **8**, 1467

www.rsc.org/softmatter

PAPER

Self-assembled multilayers of modified ITO in polymer solar cells by soft-imprinting

Li-Chen Huang,[ab] Hung-Wei Liu,[c] Chin-Wei Liang,[c] Tsu-Ruey Chou,[ab] Leeyih Wang*[cd] and Chih-Yu Chao*[ab]

Received 27th September 2011, Accepted 7th November 2011
DOI: 10.1039/c1sm06837g

Optimized performances of polymer solar cells has been of magnificent interest in recent years. A variety of approaches have been reported to alter or replace the polymer buffer layers in solar device structures. In this present work, surface modification of indium tin oxide (ITO)-coated substrates through the use of self-assembled multilayers by the soft-imprinting method has been applied to adjust the anode work function and device performance in polymer solar cells based on a P3HT:PCBM heterojunction. The efficiency and morphology of the solar device with CF_3-terminal group materials as a buffer layer have been measured and investigated. These results demonstrate that the soft-imprinting method is an effective and rapid procedure that enhances the quality of polymer solar cells and indicates potential implications for other organic devices containing an interface between a blended organic active layer and an electrode layer.

1. Introduction

Organic photovoltaic (OPV) cells hold great promise for clean energy generation by converting sunlight into electricity since solar power is an abundant energy source and can be used anywhere.[1] In particular, it provides relatively inexpensive materials and simple solution processable substitutes to inorganic-based photovoltaic devices.[2] In addition, the advantages of using solar cell devices made from organic systems are that they possess mechanical flexibility, are light weight, and can be produced using roll-to-roll manufacturing methods at low temperatures. One of the most representative OPV cells is the device based on a blend of poly(3-hexylthiophene) (P3HT) as an electron donor and a soluble C_{60} derivative, [6,6]-phenyl-C_{61}-butyric acid methyl ester (PCBM) as an electron acceptor. Although the conversion efficiency of the conventional bulk-heterojunction (BHJ) solar cell architecture consisting of P3HT:PCBM has reached over 4–6% by a variety of processes,[3] its performance is still restrained by a relatively poor carrier transfer property, which has also impeded the path towards commercialization. Good photovoltaic devices require the optimization of phase separation and morphology formation in a blended film and also the development of new materials to allow improved interfacial contact in a balanced hole and electron charge transport. Generally, the efficiency of organic devices can be enhanced significantly when a poly(3,4-ethylenedioxythiophene):poly(styrenesulfonate) (PEDOT:PSS) layer is introduced to facilitate hole transport/injection in light-emitting diodes[4] or as a buffer layer in solar cells.[5] Nevertheless, it is well known that the indium tin oxide (ITO) glass is very sensitive to acidic environments. Due to the strong acidic nature of PSS, the aqueous solution from which the PEDOT:PSS films are cast can also be expected to etch the ITO.[6] Also, this polymer buffer layer in the organic electronic device structure can be easily oxidized in air, which leads to a deterioration in performance.

To date, many approaches, such as oxygen-plasma etching, UV-ozone treatments,[7] and self-assembling of monolayers of dipolar molecules,[8] have been delicately tailored to improve the properties of ITO substrates. Self-assembled monolayer (SAM) modification, one of the most promising methods, has been employed to alleviate this problem. It is used to insert a less air-sensitive buffer layer between the active layer and electrode in order to reduce the amount of degradation and the amount of oxygen and moisture diffusion inside the organic active layer.[9] Self-assembled monolayers of organic compounds on inorganic or metal surfaces are becoming increasingly important in many areas of material science.[10] Moreover, some research groups utilized self-organized layers as buffer layers to control the surface energy of the materials[11] and to alter the work function of the charge collecting electrodes in molecular solar cells.[12] However, the regular immersion method is incapable of producing various patterns that are designed.[13] A new strategy is desirable for the mass production of layer structures on a wide variety of substrates, which can be applicable to various fields of manufacturing, for example, microelectronics, micro-optics, and

---

[a] Department of Physics, National Taiwan University, Taipei, 10617, Taiwan. E-mail: cychao@ntu.edu.tw; Fax: +886-2-33665088; Tel: +886-2-33665130
[b] Institute of Applied Physics, National Taiwan University, Taipei, 10617, Taiwan
[c] Institute of Polymer Science and Engineering, National Taiwan University, Taipei, 10617, Taiwan
[d] Center for Condensed Matter Sciences, National Taiwan University, Taipei, 10617, Taiwan. E-mail: leewang@ntu.edu.tw; Fax: +886-2-23655404; Tel: + 886-2-33665276

organic photovoltaics. The soft-imprinting method is one very important technique to fulfil this requirement since this system provides suitable and fast experimental simplicity and flexibility for some complex work, such as organic photovoltaic devices. Furthermore, the soft-imprinting method offers a remarkable ability to form as many diverse patterns as possible.[14]

In this paper, we employed self-assembled multilayers with terminal –CF_3 groups to modify the surface characteristics of ITO substrates by the soft-imprinting method, and investigated the effects of these treatments on the morphology of the active layer, the work function of the ITO electrode and the resultant OPV performance. In BHJ solar cells using P3HT:PCBM, adjustment of surface energy and work function of ITO may lead to a tuneable morphology for the active layer and hole injection barrier reduction. As-modified ITO substrates were characterized with contact angle measurements, ultraviolet photoemission spectroscopy, UV-vis optical measurements and atomic force microscope imaging. The obtained results show that the work function of the modified ITO substrates is close to the highest occupied molecular orbital level (HOMO) of P3HT, and thus helps to reduce the barrier of hole injection. By means of CF_3-material modification, the device performances including the short-circuit current density (J_{sc}) and fill factor (F.F.) are enhanced. As a result, the CF_3-material treated sample has improved the efficiency of hole injection into the ITO and exhibited a higher power conversion efficiency, which is comparable to that of the device with a PEDOT:PSS insertion layer. Moreover, we found the soft-imprinting method which can be applied to adjust the anode work function is an efficient and fast approach for large scale flexible polymer solar cells.

2. Experimental section

A schematic diagram of the soft-imprinting method for fabricating self-assembled multilayers is illustrated in Fig. 1, and can be mainly described by the following steps. First of all, this process uses a stamp to print self-assembled multilayers onto the ITO glass in order to modify the surface properties of the ITO substrate. The soft stamp, poly(dimethylsiloxane) (PDMS), plays a crucial role in standard microcontact printing (μCP) techniques and can easily make conformal contact with different surfaces. In Fig. 1(a), wetting of the elastomeric stamp was accomplished by exposing the stamp to a 0.5 wt% solution of trimethoxy(3,3,3-trifluoropropyl)silane (CF_3–silane for short) in hexane, either by pouring the solution over the surface of the stamp or by rubbing the stamp moderately with a Q-tip which has been saturated with the CF_3–silane solution. Hydroxyl groups were introduced to the ITO substrate by carrying out O_2-plasma treatment for 15 min previously. Following the wetting step, the stamp was slowly brought into contact with the surface of ITO glass substrate in an ambient environment, as shown in Fig. 1(b). Typically, very light pressure is applied by hand in order to help complete the contact between the stamp and the surface, and to squeeze out any air bubbles. Then, the stamp was gently peeled off from the surface, as seen in Fig. 1(c). After the removal of the stamp, the CF_3–silane materials were transferred from the stamp to the ITO upon contact, and covalently bonded to the underlying ITO surface.[15] Then, the substrate was rinsed with hexane to remove the residual molecules. Eventually, the ITO substrate was sheerly modified with CF_3–silane materials, as shown in Fig. 1(d). Also, the procedure can be conducted under atmospheric pressure in an unprotected laboratory environment. The chemical structure of the CF_3–silane material is shown in Fig. 1(e). Furthermore, CF_3–silane materials exhibit many positive characteristics: ease of preparation, good stability under ambient conditions, relatively low densities of defects in the final structures, and amenability to applications in controlling interfacial properties. Herein, CF_3-layers with electron-withdrawing groups can increase the work function of the ITO/active layer interface and causes the hole injection barrier of ITO to become closer to the highest occupied molecular orbital level (HOMO) of the active layer. In many such applications, the work function of ITO has a profound effect on device performance because it affects the energy barrier height at the heterojunction interface. Subsequently, the CF_3-layer treated ITO was coated with a P3HT:PCBM blend in 1,2-dichlrobenzene (ODCB) to analyze the electrical properties of the modified ITO surfaces. Finally, a cathode comprised of stacked Ca (20 nm) and Al (100 nm) layers was evaporated onto the surface of the active layer to achieve a polymer solar cell. The complete device structure of a polymer solar cell is illustrated in Fig. 1(f).

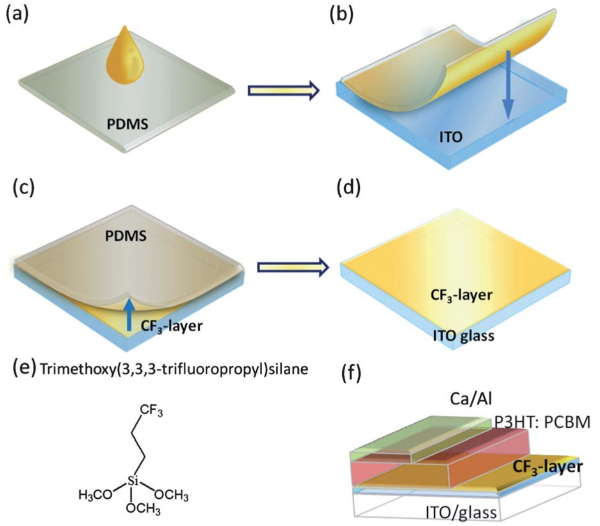

Fig. 1 Schematic representation of the formation of self-assembled multilayers by the soft-imprinting method. (a) The CF_3–silane solution was deposited on the surface of the PDMS film. (b) The CF_3–silane-coated PDMS film was inversely attached onto the ITO surface. (c) The top transparent PDMS film is peeled off from the ITO substrate. (d) After the removal of the stamp, the self-assembled multilayers of CF_3 were formed onto the ITO surface. (e) Chemical structure of the CF_3–silane material. (f) The polymer solar cell device structure consisting of ITO/CF_3-layer/P3HT:PCBM/Ca/Al.

An elastomeric stamp applied to the ITO surface is the key to the soft-imprinting method. In addition to its elasticity, the PDMS elastomer has many other benefits that make it extremely useful in the soft-imprinting process: (a) the PDMS has good chemical stability and makes conformal contact with rigid surfaces over relatively large areas. (b) The PDMS is not hydroscopic; it does not swell with humidity. (c) The PDMS elastomer has good thermal stability; prepolymers being easily molded can be cured thermally. (d) The elastomeric PDMS is durable when it is used as a stamp; we can use a PDMS stamp many times over a period of several months without observing any degradation in performance. Therefore, we chose to use the elastomeric PDMS polymer for our soft-imprinting experiments.

The PDMS stamps were prepared by cast molding: a mixture of Sylgard 184 silicon elastomer (Dow Corning) and a curing agent (10 : 1 ratio by volume). The raw material is supplied as a two-part kit: a liquid silicon rubber base (*i.e.* a vinyl-terminated PDMS) and a curing agent (*i.e.* dimethylsiloxane).[16] The two compounds were stirred in a vessel for 20 min and degassed in a centrifuge for 5 min before it was mildly poured onto the flat substrate to be solidified. In order to make a smooth surface stamp, the liquid mixture was poured onto a silicon wafer which was formerly deposited with an anti-stick solution and then it was cured at 70 °C in an oven for 4 h. The anti-stick solution is (tridecafluoro-1,1,2,2-tetrahydrooctyl)dimethulchlorosilane (FOTS) which is purchased from the Gelest company. The PDMS stamps were peeled away from the FOTS-coated silicon wafer after cooling and placed on a glass surface, they were then cut into pieces (1 cm × 1 cm). The thickness of the PDMS was around 2 to 4 mm.

For the sake of the soft-imprinting procedure, the PDMS stamps wetted with the CF_3–silane solution were usually lifted with tweezers, and softly attached to the ITO substrate to transfer the CF_3–silane materials. The 0.5 wt% CF_3–silane (Aldrich) solution was completely dissolved in a hexane solution. The ITO was first cleaned by scrubbing in a detergent, then thoroughly rinsed in deionized water, and finally sonicated in acetone and IPA. The ITO glass substrate was treated with O_2-plasma before the coating of the buffer layers in order to improve the adhesion between the ITO surface and the CF_3–silane film. For comparison, the CF_3–silane film was also replaced by PEDOT:PSS in our system as a control sample. The thickness of the CF_3–silane layer is ~6 nm which was characterized by a spectroscopic ellipsometer (J. A. Woollam VASE).

Polymer solar cells were fabricated *via* a combination of spin-coating and the soft-imprinting method on ITO glass substrates (2 cm × 2 cm). For comparison with the device using CF_3–silane treated ITO, a commonly used PEDOT:PSS (Baytron P VP AI4083) was spin-coated (40 nm) on the ITO glass, followed by heating at 140 °C for 10 min. The mixtures of P3HT (15 mg ml^{-1}) and PCBM (Nano-C, 12 mg ml^{-1}) were soluble in 1,2-dichlorobenzene (ODCB). Meanwhile, those substrates were delivered into a nitrogen-filled glove box and the P3HT:PCBM layer was later spin-coated on top of the PEDOT:PSS pre-coated ITO substrate (15 Ω $\square^{-1}$). The thickness of the active layer was *ca.* 200 nm and the device area was 0.06 cm^2, which was defined by a shadow mask. Metallic cathodes of Ca (20 nm) and Al (100 nm) were successively evaporated on it under high vacuum conditions of 10^{-6} Torr. Thermal annealing was performed at 110 °C for 10 min under a N_2 atmosphere after the deposition of the cathode. To study the performances of solar cells applying these modified ITO substrates, the current density–voltage (*J*–*V*) characteristics were measured in the dark and under AM1.5G solar illumination at an intensity of 100 mW cm^{-2}, which was obtained from a 300 W Xe lamp solar simulator (Oriel 91160) utilizing a programmable Keithley mode 2400 instrument. Light intensity was calibrated by a mono-Si reference with a KG5 filter (PV Measurements, Inc.), which was calibrated by the National Renewable Energy Laboratory.

After the imprinting process, the sample for ultraviolet photoelectron spectroscopy (UPS) measurements was stored in a vacuum desiccator and exposed briefly to the air before being placed into an ultra-high-vacuum (UHV) chamber equipped with an angle-resolved electron energy analyzer. The UPS (Thermo VG-Scientific) measurements were performed using the He **I** photo line ($h\nu = 21.22$ eV) of a He discharge lamp under UHV conditions (2×10^{-11}Torr). When the data was collected, the samples were biased at −5 V in order to measure the onset of the photoemission spectra, which was used to determine the position of the work function of the modified ITO surface. The as-treated ITO surface was also characterized by taking multiple advanced contact angle measurements (First Ten Angstron) from various locations on the substrate, which was modified with or without the CF_3–silane materials. The absorption and transmission spectra of the active layer and CF_3–silane thin film were visualized with the aid of a UV-vis spectrometer (JASCO). The morphology of the active layer surface coated on the top of the PEDOT:PSS and CF_3–silane-coated ITO was investigated under the atomic force microscope (PSIA XE-100).

3. Results and discussions

3.1 Electrode work function and surface wettability

Examples of He **I** UPS spectra of modified ITO substrates are revealed in Fig. 2, where the first derivative of the secondary-cutoff region of the UPS spectrum is shown in Fig. 2(b). The spectrum in Fig. 2(a) was taken for a sample with a −5 V bias so that the sample inelastic cutoff could be distinguished from the spectrometer. This cutoff, also called the photoemission onset, is related to the vacuum level (E_{vac}) because no electrons with less

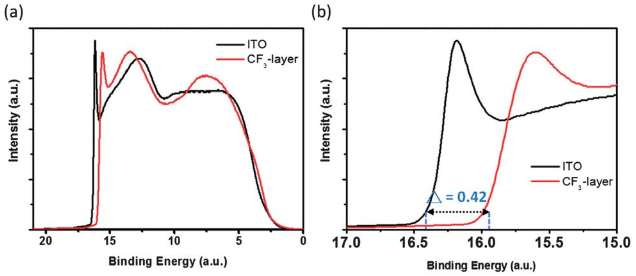

(c) O_2-Plasma (d) CF_3-silane imprinted

Fig. 2 (a) UPS spectra of the bare ITO and CF_3–silane modified ITO surfaces. (b) Close-up of the secondary electron edge (15–17 eV). Shift in binding energy is indicated as the dotted line, which is 0.42 eV. (c) The contact angle (~0°) of the O_2-plasma treated ITO substrate. (d) The contact angle of the CF_3–silane modified ITO substrate by the soft-imprinting method is 96°.

energy can escape from the solid surface.[17] The onset of photoemission corresponds to the changes in the work function at the ITO surface. The main cutoff of the secondary electron edge was used to determine the work function after each preparation step. Therefore, the work function can be calculated by subtracting the binding energy of the secondary electron edge form the He **I** excitation energy (21.22 eV).[18] As a result, through the addition of the CF_3-layer to the ITO glass substrate, a work function shift was observed. The work function of the ITO substrate in our experiment is 4.7 eV, after the O_2-plasma process. In the case of the CF_3-terminated layer, the onset of secondary electrons is 0.42 eV higher than that of the plasma treated ITO. The CF_3-layer being deposited through the soft-imprinting method, obtained a work function which is increased by 0.42 eV, to a value of 5.12 eV, which is close to the HOMO level of the active layer (~5.2 eV), and thus the hole injection barrier from the active layer to the anode is reduced. The onset of secondary electrons was determined by extrapolating two solid lines from the background and the straight onset in each spectrum. The absolute error in the determination of cut-off is estimated to be ±100 meV, while the error of spectra recorded here, relative to each other, is estimated to be smaller (about ±50 meV).

Surface modification with the CF_3–silane materials can also change the wettability of the substrate surface by replacing –OH terminal groups with fluorocarbon molecular units. Changes in wettability can affect the way it is subsequently coated with organic layers. Improved wettability results can be confirmed by measuring the static contact angle of water on treated substrates. Table 1 presents the average contact angles with ±3° uncertainty on the different ITO surfaces. The bare ITO substrate has a low water contact angle of 35°, whereas angles of nearly 0° were measured from the O_2-plasma treated ITO, as seen in Fig. 2(c). The CF_3–silane imprinted sample shows a contact angle of 96° in Fig. 2(d). An obvious increase in contact angle after the modification of ITO with the CF_3–silane materials, which primarily comes from the highly hydrophobic nature of the –CF_3 moieties, which indicates the existence of CF_3–silane on the ITO surface.

3.2 Device current–voltage characteristics

One of the critical issues concerning the high-efficiency of OPV cells, is to decrease the contact resistances of the anode and the cathode. For example, an ultrathin insulating interlayer, such as LiF, is commonly inserted between the organic active layer and the Al cathode to enhance the efficiency of electron collection.[19] In order to investigate the electrical properties of the CF_3–silane treated ITO surface, an organic solar cell composed of ITO/CF_3-layer/P3HT:PCBM blend (1 : 0.8)/Ca/Al was fabricated. The ITO substrates were modified with a layer of CF_3–silane by the soft-imprinting method. For the control device, aqueous dispersions of PEDOT:PSS after passing through a 0.45 μm PVDF filter were spun at 3500 rpm for 30 s on top of clean ITO substrates. The subsequent active layer was prepared the same way as the sample with a CF_3–silane buffer layer. All electrical measurements and active layer fabrications were conducted inside a glove box in which the condition is less than 1 ppm O_2 and 1 ppm H_2O. Fig. 3 shows the illuminated current density–voltage (*J*–*V*) curves of the P3HT:PCBM material devices fabricated on ITO (w/o buffer layer), PEDOT:PSS-coated ITO and CF_3–silane modified substrates.

Table 1 Static contact angle measured for ITO anodes treated in a variety of processes

Anode	Contact angle [°]
Untreated	35
O_2 plasma	~0
CF_3–silane imprinted	96

Without the aid of the inserted buffer layers, such as PEDOT:PSS or CF_3–silane, the device performance shows poor results compared with the devices with buffer layers. On the other hand, the series resistance (R_s) of different buffer layers at a given voltage (*c.a.* 1 V) decreases from 8.4 Ω cm^2 (PEDOT:PSS) to 3.4Ω cm^2 (CF_3–silane), which emphasized that the interfacial formation is enhanced in the CF_3-layer devices. The corresponding power conversion efficiency (PCE) increases from 3.18 ± 0.16% (PEDOT:PSS) to 3.42 ± 0.27% (imprinted). The performance parameters of all samples are summarized in Table 2. As expected, the F.F. value increases from 60.4 ± 0.5 for the PEDOT:PSS-coated device to 63.4 ± 0.5 for the CF_3–silane imprinted device, indicating a reduction in the effective series resistance, whilst the open-circuit voltage remains almost the same. Moreover, work function shifts have virtually no effect on the open-circuit voltage (V_{oc}), which is in accordance with the idea that V_{oc} is controlled intrinsically by the difference between the lowest unoccupied molecular orbital (LUMO) energy level of the acceptor and the HOMO energy level of the donor, and is insensitive to the electrode work functions.[20] As both J_{sc} and F.F. values increase with decreasing interfacial energy differences for the CF_3–silane modified device, this energetic behavior is very likely to be responsible for the behavior observed here. The *J*–*V* curves of all devices under simulated AM 1.5 illumination show J_{sc} and F.F. increase in the CF_3–silane imprinted sample. This again corresponds to the decreased R_s value. As a result, the CF_3–silane treated sample has improved the efficiency of hole injection into the ITO and exhibited a higher power conversion efficiency comparable to that of the device with a PEDOT:PSS insertion layer.

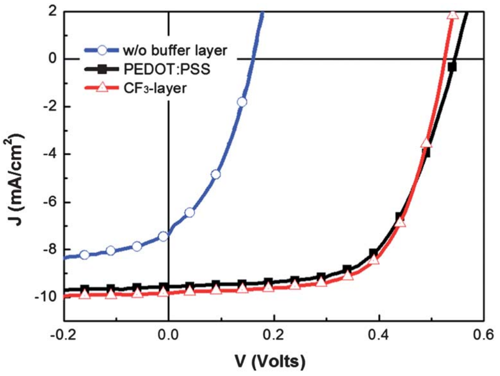

Fig. 3 *J*–*V* characteristics of P3HT:PCBM bulk heterojunction devices w/o a buffer layer (circle line), with PEDOT:PSS (square line) and the CF_3-layer (triangle line) under simulated AM 1.5 irradiance (100 mW cm^{-2}).

Table 2 Summary of the performance parameters of the P3HT:PCBM based solar cells with and without a PEDOT:PSS layer compared with the CF_3-layer device

Buffer materials	V_{oc} (V)	J_{sc} (mA cm^{-2})	F.F. (%)	PCE (%)
w/o	0.17	7.37	35.1	0.44
PEDOT:PSS	0.55	9.48	60.4	3.18
CF_3-layer	0.55	9.83	63.4	3.42

3.3 Absorption/transmission spectra and morphology of the active layer

The optical density of the P3HT:PCBM film and the transmission for the CF_3–silane modified ITO substrate are shown in Fig. 4. The transmission of the CF_3–silane treated ITO is slightly higher than that of the PEDOT:PSS layer in the range of 600 to 800 nm. Transparency is increased in the wavelength range where P3HT:PCBM absorbs, which makes this device suitable for applications which make full use of the solar illumination spectrum. The UV-vis spectrum is clearly illustrated in Fig. 4(b). Compared to the PEDOT:PSS-coated ITO glass, the CF_3–silane treated samples exhibit better light transmission characteristics in the visible light spectrum and can efficiently reduce the loss of light passing through the solar device. In addition to reaching relatively low optical absorption, the fluorocarbon surfaces exhibit quite high transparency values throughout the visible light range, which is important for the application of a transparent electrode material.

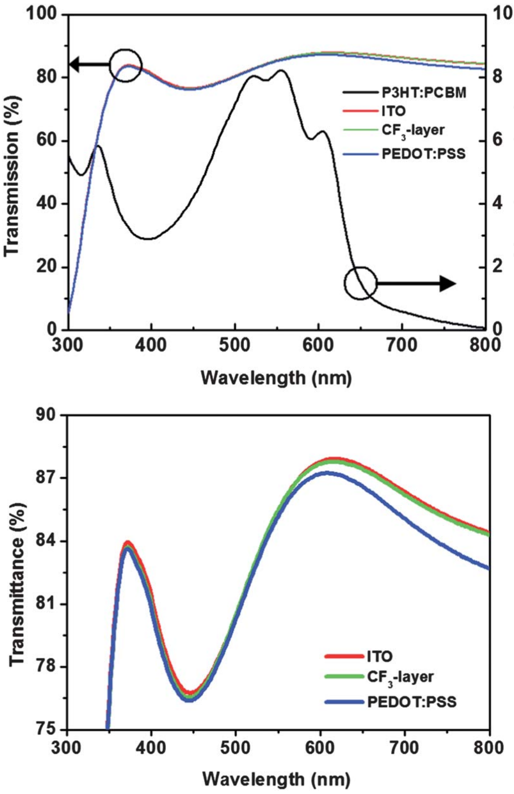

Fig. 4 Transmission of various buffer layers and absorbance of the P3HT:PCBM material in UV-vis spectra. (a) The left axis represents the transmission ratios of different buffer layers; the right axis is the UV-vis absorption spectra for the film of P3HT:PCBM (in 1 : 0.8 wt/wt ratios). (b) The transmission spectrum for the fluorocarbon layer between 610 and 800 nm is larger than that of the PEDOT:PSS-coated surface.

In order to further validate the surface modified imprinting process, the phase image and topography of the subsequently coated active layer is investigated. In Fig. 5, the morphology of the active layers on the CF_3–silane treated ITO substrates shows a more uniform distribution of P3HT and PCBM than on the PEDOT:PSS surface after annealing. As can be seen in Fig. 5(a) and (b), the CF_3–silane treated surface could provide optimized phase separation of the P3HT:PCBM blend film due to the hydrophobic surface of the CF_3 film. The dark region refers to PCBM-rich areas; the bright area indicates the P3HT materials. As a result, the surface roughness of each sample is 4.57 nm (PEDOT:PSS/ITO) and 3.62 nm (CF_3–silane treated ITO), respectively, as shown in Fig. 5(c) and (d). The lower surface roughness indicates an increase in the number of interfaces between the donor and the acceptor. The increased interfaces are beneficial to the exciton charge separation and charge transportation which mostly contributes to the J_{sc}. The rough surface is a signature of P3HT self-organization, which increases the ordered structure formation in the active film.[2] Consequently, there is no excessive phase separation observed in the CF_3-sample, which means a better device performance using CF_3–silane imprinting is plausible. Rough surface morphology of the blend film may induce poorer contact between the active layer and cathode. Therefore, the CF_3–silane treated sample has optimised the active layer morphology and was found to have better performance than that of the device with a PEDOT:PSS insertion layer. The CF_3-layer serves as a passivation of inorganic surface trap states, improving the exciton dissociation efficiency at the polymer/active interface, as well as a template to influence the overlayer BHJ distribution of phase morphology, leading to better charge selectivity and enhanced solar cell performance.[21]

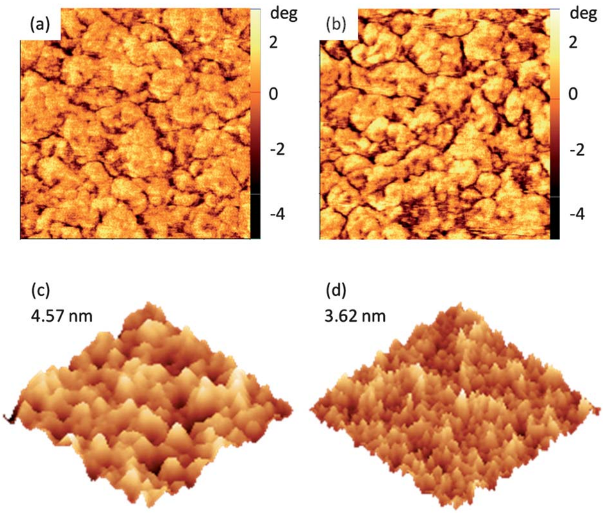

Fig. 5 Phase images of the P3HT:PCBM layer after annealing were observed under an AFM system. (a), (b): The phase images. (c), (d):The surface roughness of the active layers coated on the standard (PEDOT: PSS) and CF_3–silane treated ITO surfaces, respectively. (AFM image dimensions: 5 μm × 5 μm).

4. Conclusions

The soft-imprinting method offers immediate and fast advantages in applications in which photolithography falters or fails. In summary, we have successfully proved the feasibility of the soft-imprinting method which we applied to organic solar cell devices. We note that some of these SAM-treated devices cannot easily be fabricated using existing techniques based on the conventional immersion method. In our work, the obtained power conversion efficiency (PCE) in the absence of a PEDOT:PSS layer was 3.42% for a CF_3–silane treated surface, which is higher than the corresponding PCE 3.18% of OPV cells (with PEDOT:PSS). As a result, a significant decrease in series resistance was observed in the device with a CF_3-layer. We also found that, by means of such CF_3–silane modification, both the J_{sc} and F.F. values are enhanced as compared to those of common OPV devices with PEDOT:PSS as a buffer layer. By carrying out further investigations into applications for this technique, we expect to extend this fast fabrication technique to the large scale fabrication of layer structures and to the flexible polymer solar cell industry.

Acknowledgements

The authors CYC and LW would like to thank the National Taiwan University, Academia Sinica, National Science Council, and Ministry of Education of the Republic of China for financial support on this work.

Notes and references

1 G. Yu, J. Gao, J. C. Hummelen, F. Wudl and A. J. Heeger, *Science*, 1995, **270**, 1789; J. Brabec, N. S. Sariciftci and J. C. Hummelen, *Adv. Funct. Mater.*, 2001, **11**, 15.

2 G. Li, V. Shrotriya, J. Huang, Y. Yao, T. Moriarty, K. Emery and Y. Yang, *Nat. Mater.*, 2005, **4**, 864.

3 W. L. Ma, C. Y. Yang, X. Gong, K. H. Lee and A. J. Heeger, *Adv. Funct. Mater.*, 2005, **15**, 1617; Y. Y. Kim, S. Cook, S. M. Tuladhar, S. A. Choulis, J. Nelson, J. R. Durrant, D. D. C. Bradley, M. Giles, I. McCulloch, C.-S. Ha and M. Ree, *Nat. Mater.*, 2006, **5**, 197; G. Zhao, Y. He and Y. Li, *Adv. Mater.*, 2010, **22**, 4355.

4 A. Elschner, F. Bruder, H.-W. Heuer, F. Honas, A. Karbach, S. Kirchmeyer, S. Thurm and R. Wehrmann, *Synth. Met.*, 2000, **139**, 111–112.

5 J. Y. Kim, K. Lee, N. E. Coates, D. Moses, T.-Q. Nguyen, M. Dante and A. J. Heeger, *Science*, 2007, **317**, 222.

6 M. P. de Jong, L. J. van IJzendoorn and M. J. A. de Voigt, *Appl. Phys. Lett.*, 2000, **77**, 2255.

7 H. K. Lee, J. K. Kim and O. O. Park, *Org. Electron.*, 2009, **10**, 1641.

8 Y. Vaynzof, D. Kabra, L. Zhao, P. K. H. Ho, A. T.-S. Wee and R. H. Friend, *Appl. Phys. Lett.*, 2010, **97**, 033309.

9 K. W. Wong, H. L. Yip, Y. Luo, K. Y. Wong, W. M. Lau, K. H. Low, H. F. Chow, Z. Q. Gao, W. L. Yeung and C. C. Chang, *Appl. Phys. Lett.*, 2002, **80**, 2788.

10 G. M. Whitesides, J. P. Mathias and C. T. Seto, *Science*, 1991, **254**, 1312.

11 Q. Wei, T. Nishizawa, K. Tajima and K. Hashimoto, *Adv. Mater.*, 2008, **20**, 2211.

12 S. Khodabakhsh, B. M. Sanderson, J. Nelson and T. S. Jones, *Adv. Funct. Mater.*, 2006, **16**, 95.

13 B. de Boer, A. Hadipour, M. M. Mandoc, T. van Woudenbergh and P. W. M. Blom, *Adv. Mater.*, 2005, **17**, 621.

14 B. D. Gates, Q. B. Xu, M. Stewart, D. Ryan, C. G. Willson and G. M. Whitesides, *Chem. Rev.*, 2005, **105**, 1171.

15 D. L. Angst and G. W. Simmons, *Langmuir*, 1991, **7**, 2236.

16 Y. Xia and G. M. Whitesides, *Annu. Rev. Mater. Sci.*, 1998, **28**, 153.

17 A. Kahn, N. Koch and W. Gao, *J. Polym. Sci., Part B: Polym. Phys.*, 2003, **41**, 2529.

18 D. M. Alloway, M. Hormann, D. L. Smith, N. E. Gruhun, A. L. Graham, R. Colorado, V. H. Wysocki, T. R. Lee, P. A. Lee and N. R. Armstrong, *J. Phys. Chem. B*, 2003, **107**, 11690.

19 C. J. Brabec, S. E. Shaheen, C. Winder and N. S. Sariciftci, *Appl. Phys. Lett.*, 2002, **80**, 1288; E. Ahlswede, J. Hanisch and M. Powalla, *Appl. Phys. Lett.*, 2007, **90**, 163504.

20 C. J. Brabec, A. Cravino, D. Meissner, N. S. Sariciftci, T. Fromherz, M. T. Rispens, L. Sanchez and J. C. Hummelen, *Adv. Funct. Mater.*, 2001, **11**, 374.

21 S. K. Hau, H. L. Yip, O. Acton, N. S. Back, H. Ma and A.-Y. Jen, *J. Mater. Chem.*, 2008, **18**, 5113.